Proceedings of the IASS 2024 Symposium
Redefining the Art of Structural Design
August 26-30, 2024, Zurich Switzerland
Philippe Block, Giulia Boller, Catherine DeWolf,
Jacqueline Pauli, Walter Kaufmann (eds.)

Form-finding and structural modeling of membrane-tensegrity composite structures with proposal for highly feasible model

Yohei NAGANO*, Takuo NAGAI[a]

* Azusa Sekkei Co., Ltd.
MFIP Haneda F3, 10-11 Haneda Asahi-cho, Ohta-ku, Tokyo, Japan
nagano-y@azusasekkei.co.jp

[a] Department of Design and Architecture, The University of Shiga Prefecture

Abstract

Membrane-tensegrity composite structures have outstanding characteristics such as lightweight, simple assembly, and compact storage for transportation. However, due to the significant variation in the tensile stress applied to the membrane material, it is challenging to model membrane material appropriately and accurately understand the overall structure's equilibrium shape and stiffness. Therefore, we investigate some analysis methods using a simple model of membrane-tensegrity composite structures and verify the validity of the analysis methods by comparing the real behavior with the analysis results. We modeled the membrane-tensegrity composite structure by replacing the membrane material with truss elements based on a physical model, conducted tensile tests of the membrane materials adapted to the replacement method, and performed form-finding using the dynamic relaxation method. Furthermore, we aimed at the application to real buildings and devised a more stable membrane-tensegrity composite structure with Y-shaped compression members. We also confirmed that the analysis method of this study could be applied to this model.

Keywords: tensegrity, membrane structure, form-finding, stiffness evaluation, physical model experiment

1. Introduction

The current construction industry occupies a very large proportion in terms of the use of fossil resources, the emission of industrial waste, and the emission of greenhouse gases, and there is a demand for reducing these environmental impacts and transforming into a sustainable industrial structure. R. Buckminster Fuller (1895-1983) is one of the few pioneers who quickly raised this issue in the architectural field in the last century. He has been involved in the development and proposal of various lightweight structures from the perspectives of resource saving and reducing environmental impact, and the tensegrity structure is one of them.

Tensegrity is a structural system that utilize continuous tensile forces and discontinuous compressive forces, and they stabilize by introducing initial tension into the tensile members. Replaced multiple tensile elements of tensegrity structures with a single membrane material are membrane-tensegrity composite structures. A notable example is the “MOOM Pavilion” designed by C+A [1]. This design demonstrates advantages such as lightweight construction, straightforward assembly, and compact storage for transportation. However, the membrane material in membrane-tensegrity composite structures does not form minimal surfaces, and there is significant variation in tensile stress on the membrane. Because of the above, it is challenging to model the membrane material appropriately when creating analysis models. Therefore, membrane-tensegrity composite structures present challenges in grasping the equilibrium shape and evaluating the overall stiffness. While there are some studies on the equilibrium shape and stability of membrane-tensegrity composite structures ([2]-[4]), there is little

research on methods for evaluating the stiffness and behavior subjected external loading (e. g. Tan et al. [5]). Considering the application to real structures, it is important to establish an analysis method that can accurately capture the behavior under external forces. Therefore, the authors have been conducting research aimed at establishing a simple and accurate method for evaluating stiffness by replacing membrane materials with truss elements.

In our previous research [6], we investigated the analysis method using a simple model with compression members in one direction (plane arch model), as shown in Fig. 1, and we confirmed the effectiveness of the analysis methods by comparing the real behavior with the analysis results. As a result, we found that we could accurately determine the equilibrium shape using the proposed analysis method but could not accurately grasp the behavior under external forces. Therefore, in this study, we improved the modeling method for membrane materials and demonstrated the validity of the analysis method by comparing the real behavior with the analysis results again. Moreover, we found that the model used for investigating the analysis method shown in Fig. 1 was very unstable, and it was difficult to conduct studies on a larger scale. Therefore, we devised a more stable membrane-tensegrity composite structure with Y-shaped compression members (YC model) and confirmed whether the analysis method of this study could be applied to the YC model as well.

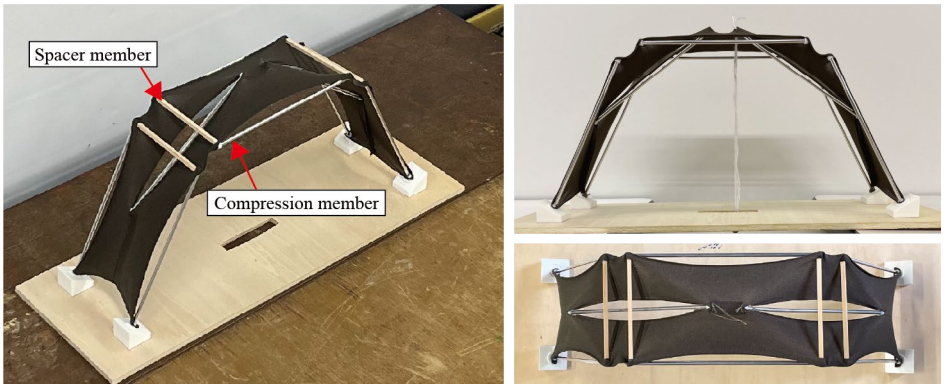

Figure 1: Photos of physical model (plane arch model).

2. Form-finding method of plane arch model

2.1. Making method of physical model

Fig. 2 shows the making method for the plane arch model (shown in Fig. 1). To create a cutting diagram (natural condition) of membrane material, we created a 3D model according to geometric rules, as shown in Fig. 2(a). We set the compression members to the position of the sides of a regular polygon and determined their length by extending each side of the polygon based on the central angle θ. Then, by rotating the compression members as shown in the diagram, we unfolded the 3D model into the plane, created a simple rectangular development diagram, and created a cutting diagram by scaling down the development diagram (Fig. 2(b)). In the cutting diagram, the X-direction corresponds to the warp direction of the membrane material, the Y-direction corresponds to the weft direction, and the compression members are parallel to the X-direction. Here, the cutting diagram was created by scaling down the development diagram to 0.65 times in both directions. We made the compression members for the same length as in the 3D model and the development diagram, and created the membrane material according to the cutting diagram. Finally, by inserting the compression members into the cut membrane material and pulling both ends until they reach the same value as the span of the 3D model (Fig. 2(c)), and we introduced tension into the membrane material. However, as we scaled down the membrane material in both directions, we could not keep the span between the adjacent compression materials, and thus, we could not successfully introduce tension into the membrane material. Therefore, as shown in Fig. 1, we inserted the spacer members to constrain the span between the compression materials in the Y-direction and introduce tension into the membrane material.

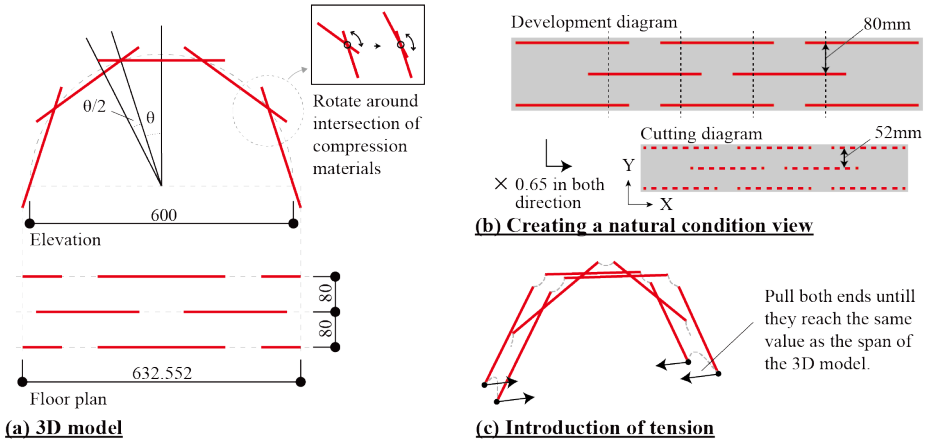

Figure 2: Making method of physical model of plane arch model.

2.2. Replacement method of membrane material

In this study, we aimed to model the membrane material as simple and accurate as possible. We replaced the membrane material with truss elements (equivalent membrane elements; EMEs) by connecting parts of the membrane material where tension forces particularly act with straight lines concerning the physical model, as shown in Fig. 3(a). However, setting the stiffness and cross-sectional shape of the EMEs based on visual information obtained from the physical model was difficult. Therefore, in this study, we attempted to determine the properties of the EMEs by conducting tensile tests on the membrane material adapted to the replacement method.

Fig. 3(b) presents the analysis model created by replacing the membrane material with EMEs. If we use the replacement method shown in Fig. 3(a), two models can be considered: “without intersections,” the crossing of EMEs is not considered, and “with intersections,” the crossing of EMEs is considered. In the analysis model “with intersections,” EMEs that cross each other share a node, as shown in the figure, and transmit the tension to each other. We conducted form-finding using these two models. Moreover, in parts where we inserted spacer members in the physical model, we restrain the movement in the Y-axis direction of eight points on both sides, as shown in Fig. 3(b), so that we can prevent the reduction in width between the adjacent compression members, the same as the physical model.

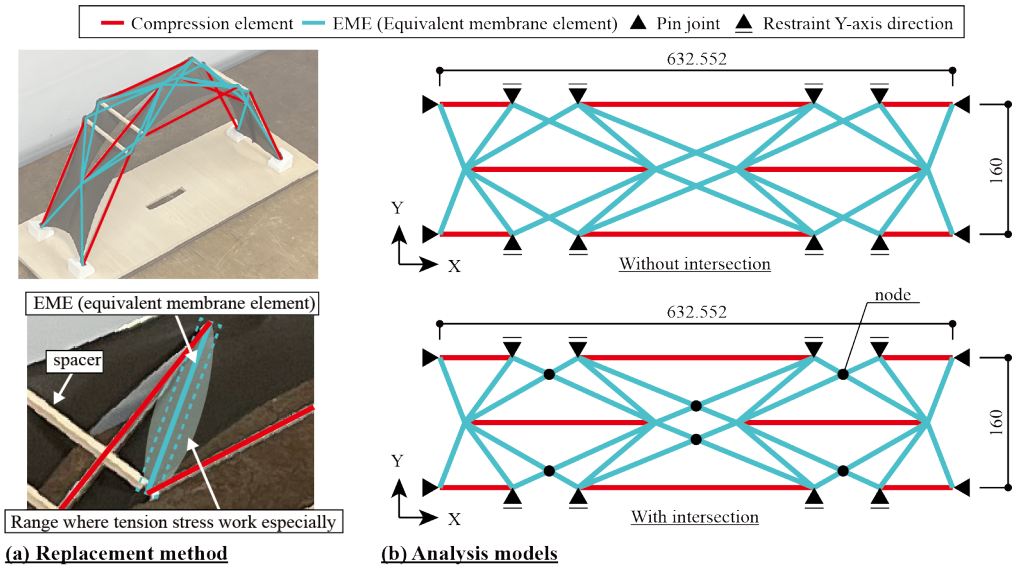

Figure 3: (a) Replacement method, (b) Analysis models.

2.3. Tensile test of membrane material

To examine the load-strain relationship of the EMEs, we conducted tensile tests by pulling two points at both ends of the membrane material similar to the physical model. As shown in Fig. 4(a), we cut out test pieces in the direction of the EMEs. The test pieces in the direction of EME A (angle θ_A) are labeled A1, and the test pieces in the direction of EME B (angle θ_B) are labeled B1 (θ_A is 23.34 degrees concerning the warp direction, and θ_B is 37.21 degrees). Furthermore, to match the boundary conditions of the physical model and the test pieces, we glued fixtures of the same diameter as the physical model's joints (10 mm) to both ends of the test pieces and conducted the tensile test (Fig. 4(b)). After conducting several tests with varying widths of the test pieces, we found that increasing the width beyond 60 mm did not alter the load-strain relationship. Therefore, we fixed the width at 60 mm for the fabrication of the test pieces. This tensile test is a uniaxial tensile test (Fig. 4(c)).

On the other hand, in the equilibrium states of the membrane-tensegrity composite structures, tensile forces act in various directions within the membrane material, not just in one direction. Therefore, it is unclear whether we can accurately estimate the stiffness of the EMEs using the load-strain relationship equations for directions A and B of the EMEs determined by the uniaxial tensile test. Hence, as shown in Fig. 4(d), we applied initial tension stress to the orthogonal direction of the axis of the test pieces by inserting rods, and we conducted a tensile test. We can predict that the load-strain relationship of EMEs will change depending on the length of the inserting rod, but it is difficult to predict how much tension will act in the orthogonal direction of the EMEs in the real model. Therefore, we set the length of the rod according to the same method of making the physical model, as shown in Fig. 4(d). By doing that, we created test pieces that act roughly the same tensile stress as real phenomena in the orthogonal direction. This tensile test is a biaxial tensile test, and the test piece in the direction of EME A (angle θ_A) is labeled A2, and the test piece in the direction of EME B (angle θ_B) is labeled B2.

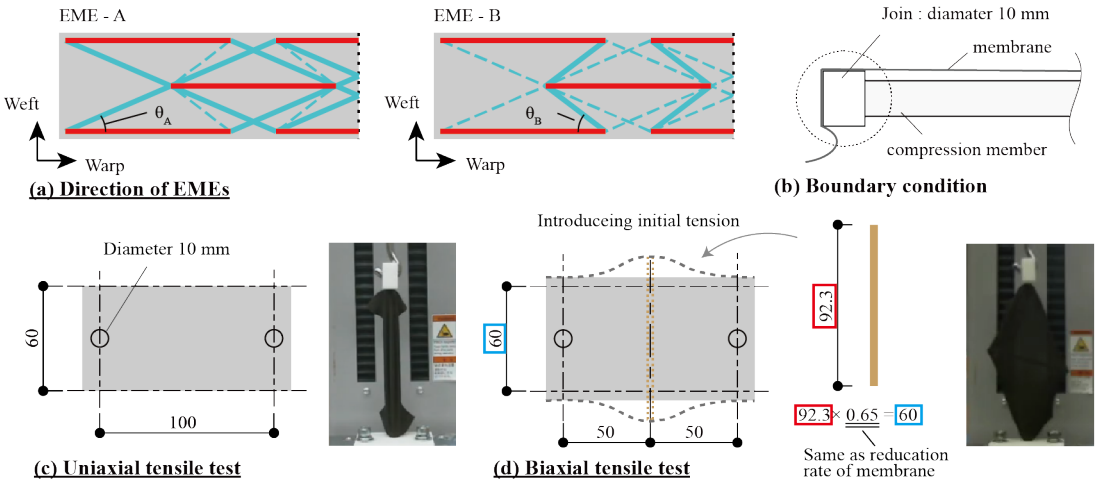

Figure 4: Method of tensile tests

Fig. 5 shows the load-strain relationships obtained by the least squares method from the tensile test results. We compared the results of the uniaxial tensile test with the biaxial tensile test, as shown in the figure. We can confirm that the results of the biaxial tensile test showed higher stiffness than those of the uniaxial tensile test. The load-strain relationship equations obtained from the results of the uniaxial tensile test are Eq. (1) and Eq. (2), while those obtained from the biaxial tensile test are Eq. (3) and Eq. (4). We tried to use these equations to perform form-finding using the dynamic relaxation method (Zhang and Ohsaki [7]) and compared the real behavior with the analysis results.

$$S_{A1}(\varepsilon) = 8.6\varepsilon^5 - 11.3\varepsilon^4 + 12.7\varepsilon^3 - 2.3\varepsilon^2 + 6.6\varepsilon \quad [\mathrm{N}] \tag{1}$$

$$S_{B1}(\varepsilon) = 12.9\varepsilon^5 - 30.1\varepsilon^4 + 34.4\varepsilon^3 - 14.0\varepsilon^2 + 8.7\varepsilon \quad [\mathrm{N}] \tag{2}$$

$$S_{A2}(\varepsilon) = 18.1\varepsilon^5 - 40.2\varepsilon^4 + 47.8\varepsilon^3 - 18.8\varepsilon^2 + 10.9\varepsilon \quad [\mathrm{N}] \tag{3}$$

$$S_{B2}(\varepsilon) = 10.2\varepsilon^5 - 25.1\varepsilon^4 + 33.4\varepsilon^3 - 15.6\varepsilon^2 + 10.2\varepsilon \quad [\mathrm{N}] \tag{4}$$

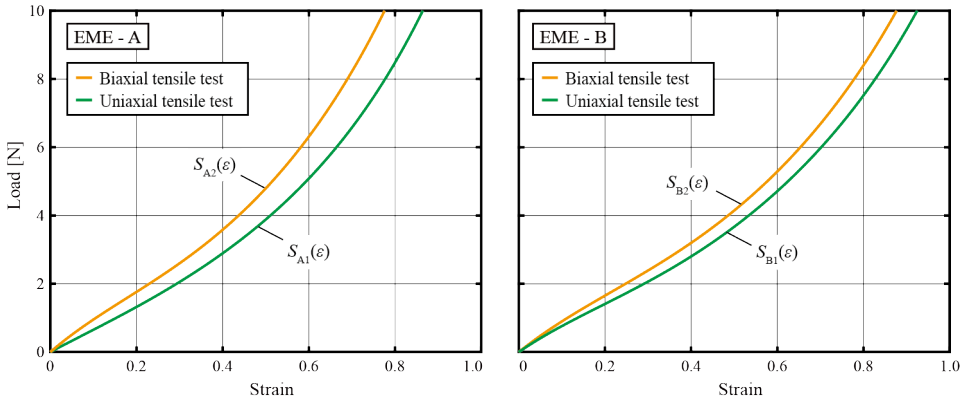

Figure 5: Tensile test results.

In our previous research [6], we also conducted biaxial tensile tests using fixtures with a diameter of 5 mm. By comparing the results of biaxial tensile tests using a diameter of 5 mm fixtures with those using a diameter of 10 mm, we examined the relationship between the adhesive area of the fixture and the stiffness of the EMEs. The results compared in Fig. 6 show that when the diameter of the fixture doubles, the load approximately doubles as well. Thus, we found that as the adhesive area between the membrane material and fixture increases, the stiffness of the EMEs also increases. Therefore, we can consider the possibility of predicting the load-strain relationship of the EMEs for the real scale model from the results of tensile tests using smaller test pieces.

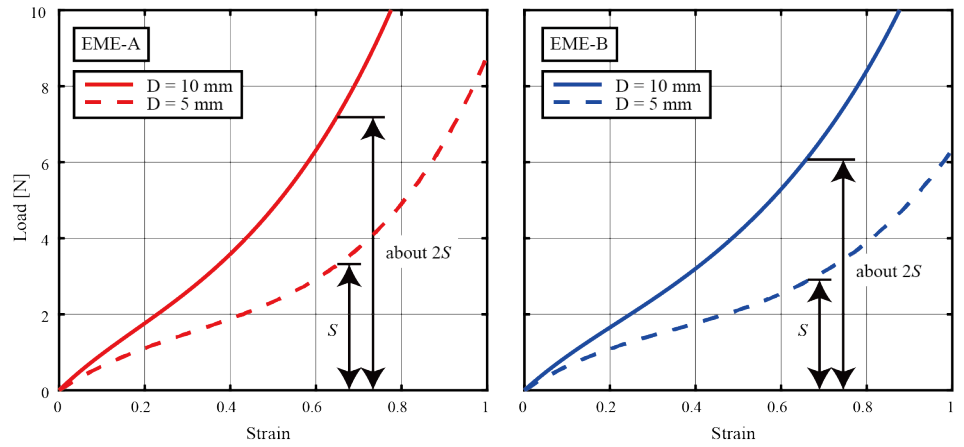

Figure 6: Relationship between the diameters of the fixtures and the stiffness of the EMEs.

3. Comparison of real phenomenon with analysis results of plane arch model

We compared the measurement result of the equilibrium shape immediately after model fabrication and the physical model experiment result with the form-finding results. In this study, we focused on two symmetric model patterns: “Model-1,” which is not considered the crossing of the EMEs and used the results of the uniaxial tensile test for the load-strain relationship equations of the EMEs, and “Model-2,” that is considered the crossing of EMEs and used the results of the biaxial tensile test for the load-strain relationship equations of the EMEs. For the self-weight, in Model-1, we evenly distributed the total weight by the nodal number and input to all the nodes, while in Model-2, the weight of the compression members was input only to the nodes at both ends of the compression elements, and we evenly distributed the weight of the membrane material and input to all the nodes.

The results of comparing the equilibrium shapes indicate that Model-2 matches the overall shape of the physical model more closely than Model-1, as shown in Fig. 7(a). Furthermore, we compared the load-displacement relationships of the experimental results with the form-finding results when we applied external forces, as shown in Fig. 7(b). From the experimental results (Fig. 7(c)), we can confirm that the behavior of Model-2 aligns very closely with the results of the physical model experiment. Additionally, while it is difficult to measure the deformed shape during the physical model experiment, we can see that the deformed shape of the analysis results and the real phenomenon are very close, as shown in Fig. 7(b) and Fig. 7(d). From these results, it is evident that considering the crossing of EMEs and using the results of the biaxial tensile test for form-finding can accurately capture the equilibrium shape and the overall stiffness.

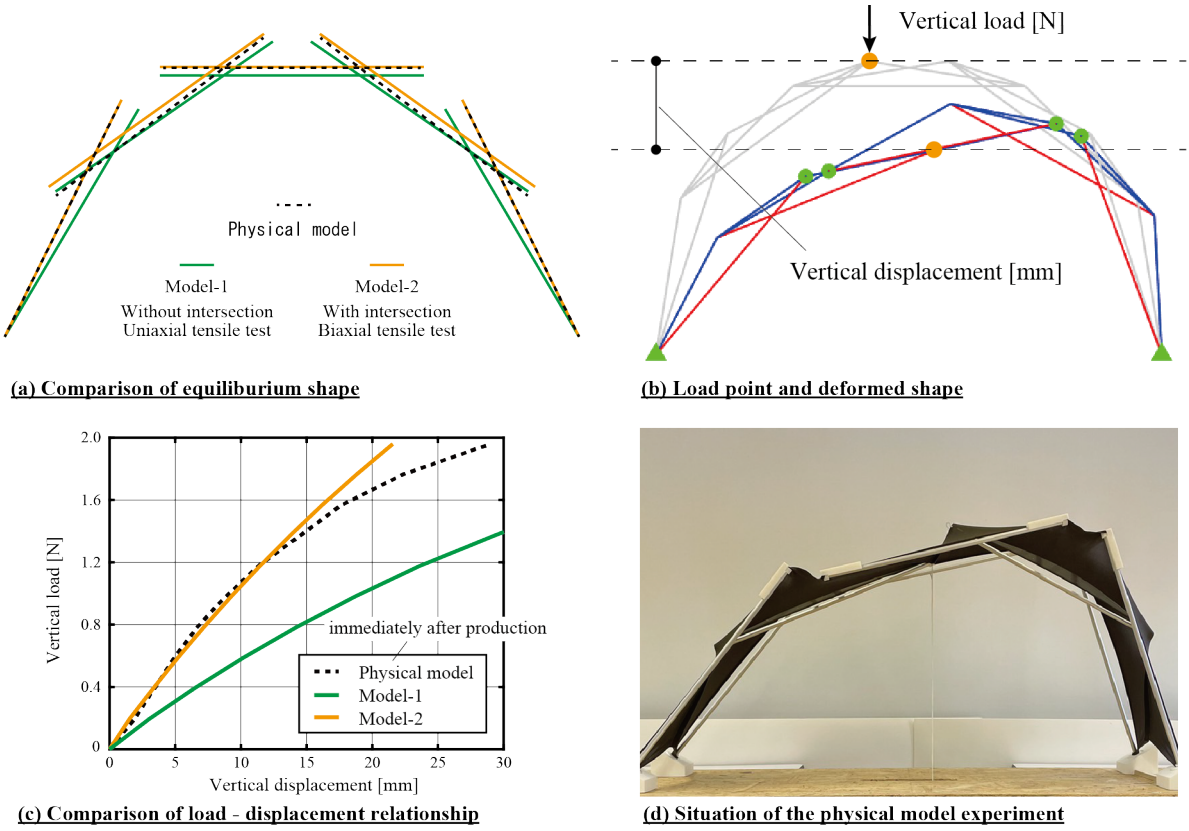

(a) Comparison of equiliburium shape

(b) Load point and deformed shape

(c) Comparison of load - displacement relationship

(d) Situation of the physical model experiment

Figure 7: Comparison of the analysis results with the real phenonenon.

4. Analysis method of Y-shaped compression model (YC model)

4.1. Making method of physical model

While the plane arch model was very simple and efficient for basic investigations and examinations of analysis methods, it was found to be highly unstable, making it difficult to consider its application to real buildings in the future. Therefore, we devised a more stable membrane-tensegrity composite structure with Y-shaped compression members. Fig. 8(a) shows the photos of the physical model. This model is the YC model. To facilitate the examination of modeling methods of the membrane material and the understanding of mechanical properties, we created a large model as simple as possible. The arrangement pattern of the compression members was determined by placing equilateral triangles on the plane, as shown in Fig. 8(b). We inserted the Y-shaped compression members bigger than the triangles on the cutting diagram (Fig. 8(c)), and introduced tension into the membrane material by pulling the three points marked with black circles on the cutting diagram to the center and assembled the model.

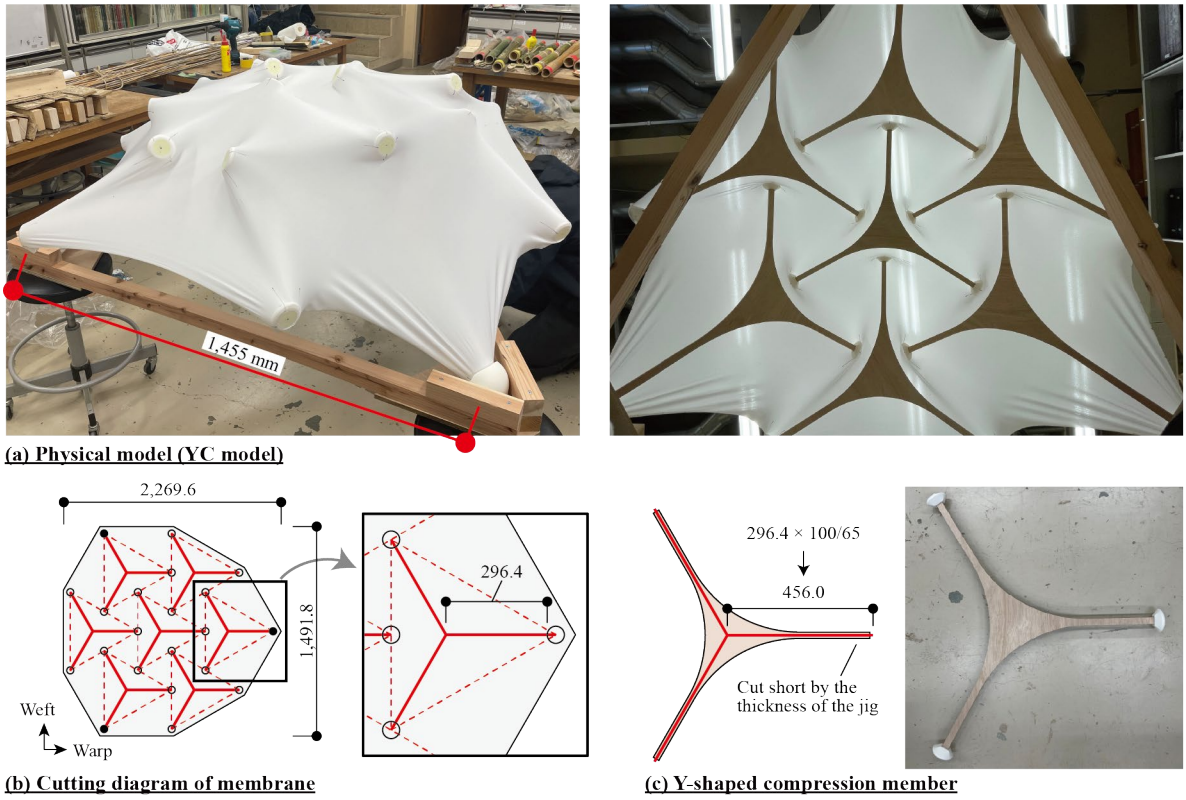

Figure 8: Physical model and creating method of YC model.

4.2. Replacement method of membrane material

For the YC model, we performed form-finding by applying the analysis method from Ch. 2 and comparing the results with the real behavior. While we cannot directly apply the replacement method of membrane material from Sec. 2.2 to the YC model, we observed that when only one side of the equilateral triangle on the cutting diagram is displayed, it matches the pattern of compression members in the plane arch model, as shown in Fig. 9. Therefore, by connecting EMEs using the same method as the plane arch model and performing the replacement method for all three sides, we could replace the membrane material with EMEs, as shown in the figure. Although overlapping EMEs occur, we treated them as a single element, and we performed the replacement method considering the intersection of EMEs. Additionally, to simplify calculations, we replaced the Y-shaped compression members with equilateral triangles for form-finding.

We obtained the load-strain relationship equations for the EMEs using the biaxial tensile test described in Sec. 2.3. We performed form-finding using the dynamic relaxation method [7] and compared the results of form-finding with the real behavior.

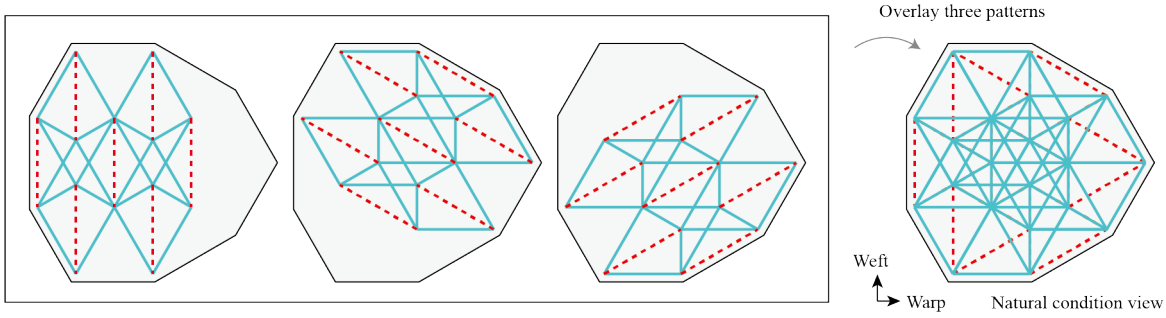

Figure 9: Replacement method of membrane material with EMEs.

4.3. Biaxial tensile test

To determine the load-strain relationship of EMEs for the YC model, we also conducted biaxial tensile tests aligned with the direction of the EMEs. However, due to the physical model's fixture having a diameter of 50 mm in the adhesive area, it was difficult to perform tensile tests on test pieces made to match the diameter of the adhesive area. Therefore, based on the results from Sec. 2.3, we tried to conduct biaxial tensile tests using test pieces glued with 10 mm diameter fixtures, multiply the load of the test results by five, and determine the load-strain relationship for the EMEs of the YC model.

In the YC model, there are four directions for the EMEs: A is at 0 degrees (in the warp direction), B at 30 degrees, C at 60 degrees, and D at 90 degrees (in the weft direction). Fig. 10 shows the results of the biaxial tensile tests. Since the diameter of the physical model's joint adhesive area is five times that of the diameter of the tensile test fixture, we can estimate the load-strain relationships of the EMEs by multiplying tensile test results five times. Eq. (5)-(8) are the load-strain relationship equations multiplied by five, and we used these equations for form-finding.

$$S_{\mathrm{A2}}(\varepsilon) = 4.3\varepsilon^5 + 15.2\varepsilon^4 - 28.1\varepsilon^3 + 43.6\varepsilon^2 + 17.9\varepsilon \quad [\mathrm{N}] \tag{5}$$

$$S_{\mathrm{B2}}(\varepsilon) = 9.8\varepsilon^5 - 15.6\varepsilon^4 + 31.6\varepsilon^3 + 15.2\varepsilon^2 + 20.2\varepsilon \quad [\mathrm{N}] \tag{6}$$

$$S_{\mathrm{C2}}(\varepsilon) = -78.9\varepsilon^5 + 317.0\varepsilon^4 - 284.1\varepsilon^3 + 133.6\varepsilon^2 + 3.3\varepsilon \quad [\mathrm{N}] \tag{7}$$

$$S_{\mathrm{D2}}(\varepsilon) = 93.8\varepsilon^5 + 61.6\varepsilon^4 - 155.4\varepsilon^3 + 124.3\varepsilon^2 - 1.9\varepsilon \quad [\mathrm{N}] \tag{8}$$

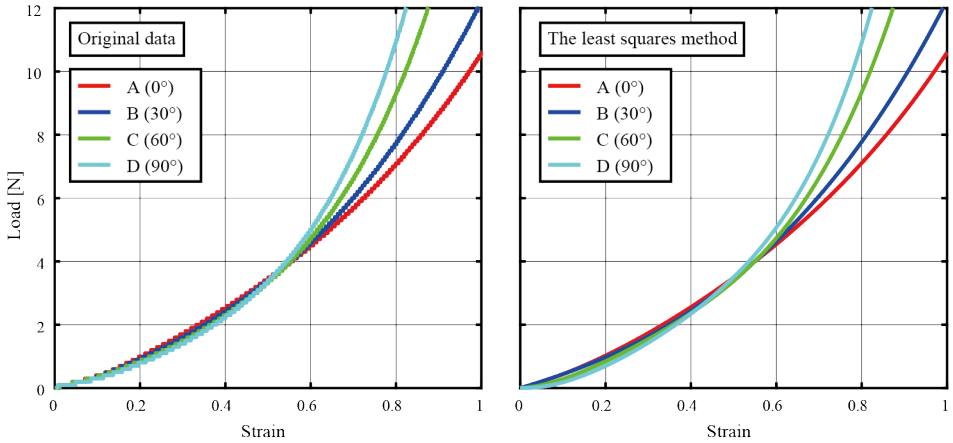

Figure 10: Biaxial tensile test results of YC model.

5. Comparison of real phenomenon with analysis results of YC model

We compared the measurement result of the equilibrium shape immediately after model fabrication with the form-finding results. For the self-weight, the weight of the compression members was evenly input to the nodes at the ends of the compression elements, and the weight of the membrane material was distributed to all nodes by dividing the membrane material as described below (Fig. 11(d)). Fig. 11(a) compares the measurement results with the analysis results that show excellent agreement in maximum height. Thus, it is evident that the proposed analysis method in this study allows for the accurate determination of equilibrium shape for membrane-tensegrity composite structures with Y-shaped compression members as well.

We conducted an eigenvalue analysis considering geometric stiffness using the stiffness of the EMEs in the equilibrium state and the initial forces acting on each member, obtained from the form-finding. To create a mass matrix, we divided the cutting diagram by the Voronoi partitioning method using the intersections of the EMEs as shown in Fig. 11(d), calculated the area of membrane material that each node covers, assumed mass concentration at the nodes, and set the nodal masses. Fig. 11(b) describes the analysis results (mode-1.) The natural period was 0.60 seconds. Furthermore, we subjected the

physical model to instantaneous acceleration, recorded on video, and measured the natural period of the physical model. Fig. 11(c) is a photo when we are shaking the physical model to induce deformation corresponding to mode-1. We measured the natural period on the video when the oscillations were minimized. As a result of the measurement, the natural period of the physical model was approximately 0.56 seconds. We found that the measurement result aligns very closely with the eigenvalue analysis results. Therefore, we confirmed that the method proposed in this study can also accurately grasp the equilibrium shape and behavior under external forces for the YC model.

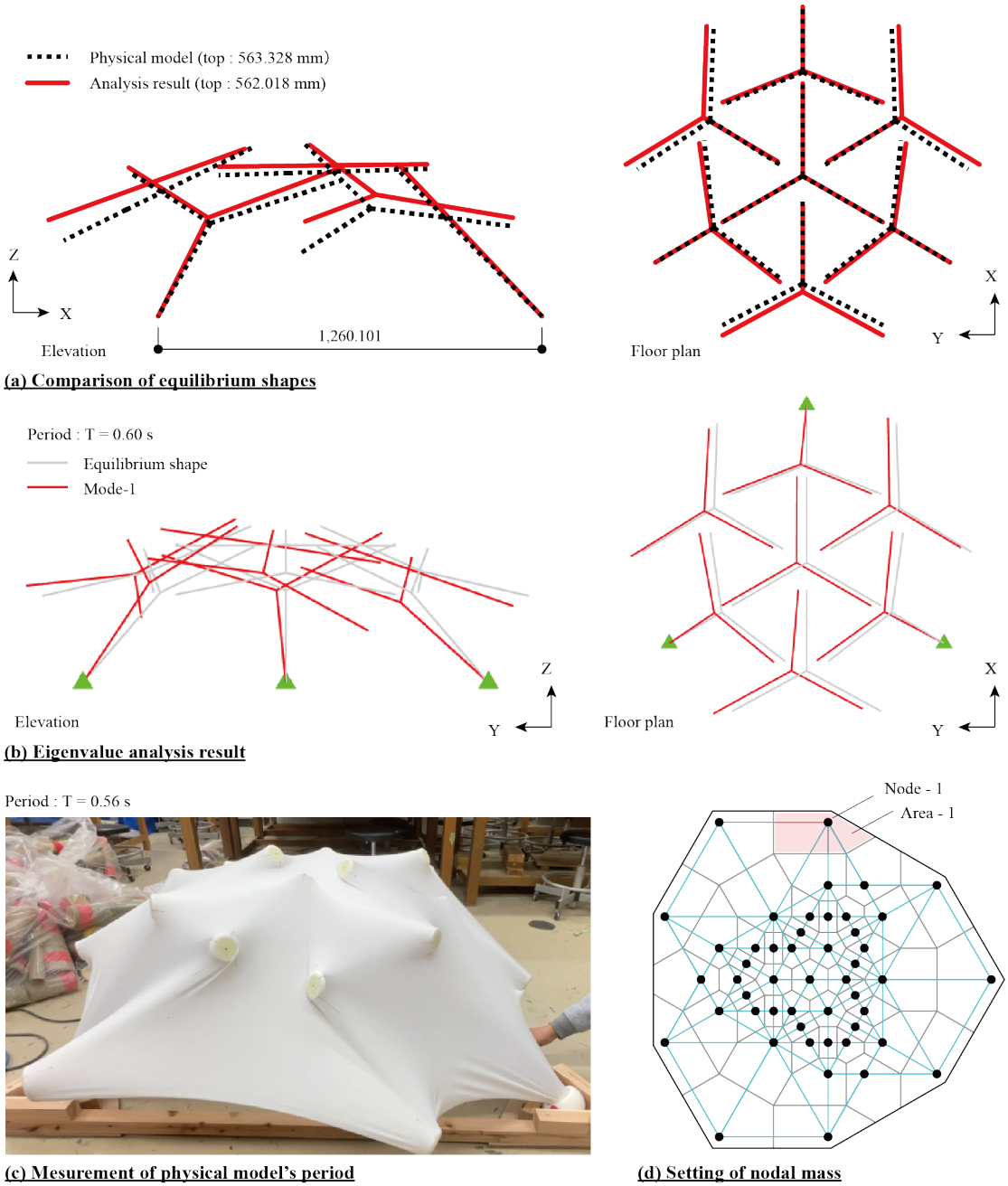

Figure 11: Comparison of the analysis results with the real phenonenon.

6. Conclusion

As a result of examining analysis methods of the membrane-tensegrity composite structures, we found that we could accurately grasp the equilibrium shape and overall stiffness of the plane arch model by replacing membrane materials with EMEs, conducting tensile tests according to the replacement method

of membrane material and performing form-finding using the dynamic relaxation method. We also found that it is necessary to replace the membrane material considering the intersection of EMEs and determine the load-strain relationship of the EMEs through biaxial tensile tests. Furthermore, from the examination results aimed at application to buildings, we observed the possibility that we can accurately grasp the equilibrium shape and overall stiffness of membrane-tensegrity composite structures with Y-shaped compression members by applying the analysis method proposed in this study.

Going forward, it is necessary to conduct mock-ups of scaled-up models and to examine methods of introducing tension into the membrane materials for application to real buildings. Additionally, to improve the accuracy of the analysis results, it is also necessary to consider the value of setting the initial tension introduced in the direction orthogonal to the axis of EMEs in biaxial tensile tests.

Acknowledgements

A portion of this research was conducted with the support of a research grant from the Nohmura Foundation for Membrane Structure's Technology. We also received valuable advice and collaboration from Dr. Masaaki Miki (The University of Tokyo), Kenji Ohya and Tatsushi Heguri (Taiyo Kogyo), Motohiro Ueda (Graduate from the University of Shiga Prefecture). We would like to express our sincere gratitude here to all those involved.

References

[1] C+A - Coelacanth and Associates, MOOM, https://c-and-a.co.jp/jp/projects/moom/, accessed 21th, Feb. 2024.

[2] M. Shigematsu, M Tanaka, H. Noguchi, "Form finding analysis of membrane-tensegrity composite structures based on variational method," *Proceedings of the 6th International Conference on Computation of Shell and Spatial Structures*, *Advances in the Optimization and Form-finding of Tensegrity Structures*, Cornell University, Ithaca, NY, USA, pp.18-21, 2008.

[3] Y. Yu and C. Lin, "Tensegric membrane structure with radiated struts," *Proceedings of the IASS Annual Symposia 2016*, *Tension & Membrane Structures*, Tokyo, Japan, pp.1-10, 2016.

[4] Y. Shimoda, K. Suto, S. Hayashi, T. Gondo, T. Tachi, "Developable Membrane-tensegrity Structures Based on Origami Tessellations," *Advances in Architectural Geometry 2023*, pp. 303-312. 2023.

[5] Y. Y. Tan, K. J. Tracy, C. Yogiaman, "Towards upscaling membrane-tensegrity shells: A design-to-fabrication workflow," *Proceedings of the IASS Annual Symposia 2023*, *Digital modelling and fabrication*, Melbourne, Australia, pp.871-880, 2023.

[6] Y. Nagano, T, Nagai, "Fundamental study on form-finding of membrane-tensegrity composite structures using a dynamic relaxation method," *Proceedings of the IASS Annual Symposium 2023*, *Integration of Design and Fabrication*, *Tension and membrane structures*, Melbourne, Australia, pp. 2199-2208. 2023.

[7] J. Zhang and M. Ohsaki, "Form-finding of complex tensegrity structures by dynamic relaxation method," *Journal of Structural and Construction Engineering*, *Architectural Institute of Japan*, Vol. 81, No. 719, pp. 71-77, 2016.